

Enhancing Imbalanced Node Classification via Curriculum-Guided Feature Learning and Three-Stage Attention Network

Abdul Joseph Fofanah, *Student Member, IEEE*, Lian Wen, *Member, IEEE*, David Chen, *Member, IEEE*, Shaoyang Zhang, *Member, IEEE*

Abstract—Imbalanced node classification in graph neural networks (GNNs) happens when some labels are much more common than others, which causes the model to learn unfairly and perform badly on the less common classes. To solve this problem, we propose a Curriculum-Guided Feature Learning and Three-Stage Attention Network (*CL3AN-GNN*), a learning network that uses a three-step attention system (*Engage*, *Enact*, *Embed*) similar to how humans learn. The model begins by engaging with structurally simpler features, defined as (1) local neighbourhood patterns (1-hop), (2) low-degree node attributes, and (3) class-separable node pairs identified via initial graph convolutional network and graph attention network (GCN and GAT) embeddings. This foundation enables stable early learning despite label skew. The *Enact* stage then addresses complicated aspects: (1) connections that require multiple steps, (2) edges that connect different types of nodes, and (3) nodes at the edges of minority classes by using adjustable attention weights. Finally, *Embed* consolidates these features via iterative message passing and curriculum-aligned loss weighting. We evaluate *CL3AN-GNN* on eight Open Graph Benchmark datasets spanning social, biological, and citation networks. Experiments show consistent improvements across all datasets in accuracy, F1-score, and AUC over recent state-of-the-art methods. The model’s step-by-step method works well with different types of graph datasets, showing quicker results than training everything at once, better performance on new, imbalanced graphs, and clear explanations of each step using gradient stability and attention correlation learning curves. This work provides both a theoretically grounded framework for curriculum learning in GNNs and practical evidence of its effectiveness against imbalances, validated through metrics, convergence speeds, and generalisation tests.

Index Terms—Curriculum Learning, Feature Learning, Attention Mechanism, Graph Neural Network, Imbalance Data, Deep Learning

I. INTRODUCTION

IMBALANCED datasets often lead to biased learning, where the model favours the majority class, resulting in poor performance for the minority class [1]. This issue is particularly pronounced in graph neural networks (GNNs), where the disproportionate distribution of node labels complicates the

This work was supported in part by Griffith University under Grant 58455. Abdul Joseph Fofanah, David Chen, and Lian Wen are with the School of Information and Communication Technology, Griffith University, Brisbane, 4111, Australia. (e-mail: abdul.fofanah@griffithuni.edu.au, orcid=0000-0001-8742-9325; email: l.wen@griffith.edu.au, orcid=0000-0002-2840-6884; email: d.chen@griffith.edu.au, orcid=0000-0001-8690-7196)

Shaoyang Zhang is with the School of Information and Communication Technology, Chang'an University, Xi'an, China (email: zhsy@chd.edu.cn, orcid=0000-0003-4526-9479)

Corresponding Author: abdul.fofanah@griffithuni.edu.au

attainment of high classification accuracy across all classes [2]. While curriculum learning (CL) has shown promise in machine learning tasks, existing approaches fail to address three key challenges in GNNs: (1) lack of modular architecture for progressive learning, (2) absence of clear dependencies between learning stages, and (3) inadequate integration strategies between curriculum design and GNN architecture. Traditional methods like oversampling [3] or cost-sensitive learning [4] often introduce noise or fail to capture hierarchical feature relationships in graph data.

Recent work in educational curriculum design [5] demonstrates the effectiveness of structured learning progression through three phases: *Engage* (building foundational knowledge), *Enact* (applying knowledge in context), and *Embed* (deepening understanding through practice). This framework overcomes limitations of traditional approaches by (1) providing modular learning stages that can be analysed independently, (2) establishing explicit dependencies between concepts, and (3) creating natural integration points between different knowledge levels [6], [7]. However, directly applying this to GNNs requires novel architectural innovations to handle graph-specific challenges like neighbourhood aggregation and message passing. To bridge this gap, we derive key principles from educational theory to inform our GNN design.

The rationale behind the selection of this approach “curriculum-guided feature learning network” stems from three key observations: First, human learning progresses most effectively through structured stages of increasing complexity. Second, GNNs naturally exhibit hierarchical feature learning capabilities through their layer-wise architecture. Third, class imbalance requires careful exposure control that standard training procedures cannot provide. These insights lead to a framework with five distinguishing features: (1) Modular architecture with distinct *Engage-Enact-Embed* stages, (2) clear learning progression via layer-wise dependencies, (3) stage-specific components that reflect actual functionality, (4) direct integration through network-like connections between modules, and (5) simplified configuration with module-aligned parameters, all wrapped in a *Curriculum GNN Classifier* that combines progressive architecture with adaptive curriculum loss. This synthesis of educational theory and GNN architecture enables the following stage-specific advantages.

The three-stage mechanism provides specific benefits at each level: In *Engage*, the model focuses on fundamental graph features through simplified learning objectives. *Enact*

then applies these foundations to progressively harder tasks using targeted neighbourhood sampling and attention mechanisms. Finally, *Embed* consolidates learning through deep feature integration and adaptive loss weighting. This mirrors human learning progression [8] while addressing unique GNN challenges – unlike previous CL applications in graphs [9] that treated curriculum design separately from model architecture. The result is an integrated framework where curriculum design and architectural evolution are co-optimised.

The main technical challenges involve (1) designing feature extraction layers that progressively increase receptive fields without losing local patterns, (2) implementing data embedding layers that adapt to each curriculum stage, and (3) developing attention mechanisms that dynamically weight nodes based on both curriculum progress and class distribution [10], [11]. Stage-specific gating mechanisms between modules allow controlled information flow that matches current learning objectives. This creates a coherent learning path that handles class imbalance at multiple levels while maintaining the flexibility to adapt to different graph structures and imbalance ratios.

This structured approach is crucial for imbalanced datasets because curriculum-based feature learning allows the model to first master distinguishing features of majority classes before progressively tackling more challenging minority class distinctions. Our research investigates seven key questions about curriculum learning for imbalanced GNNs: (RQ1) Whether stage-wise curriculum learning masks per-class performance disparities between minority/majority classes; (RQ2) How curriculum training compares to dynamic sampling on graphs with both label imbalance and heterophily; (RQ3) The relative contribution and interaction of each learning stage (Engage/Enact/Embed) in hierarchical feature learning; (RQ4) How modular curriculum architecture improves minority class performance versus traditional sampling; (RQ5) Whether dynamic attention mechanisms better capture minority class features than static approaches; (RQ6) The relationship between curriculum progression and optimal neighbourhood aggregation depth; and (RQ7) How performance scales with varying imbalance levels and graph structural complexity.

The three-stage mechanism (Engage, Enact, Embed) systematically aims to build robust node representations by establishing foundational feature understanding through simplified learning objectives and class-balanced sampling; applying targeted learning strategies to progressively handle more complex class boundaries and feature interactions; and deeply integrating learnt features through attention mechanisms and neighbourhood aggregation that emphasise discriminative patterns.

The main contributions of our work can be summarised as follows:

- *Modular Architecture*: Our framework decomposes the learning process into distinct, independently analysable modules (Engage, Enact, Embed) that each handle specific aspects of the curriculum progression, along with an additional feature extraction and embedding layer; the encoded representation is transformed into precise feature representations.

- *Explicit Learning Pathways*: We design the model to establish clear dependencies between layers, creating a transparent progression from simple to complex feature learning that directly addresses class imbalance at multiple levels.
- *Integrated Curriculum Strategy*: We design these modules that adaptively build directly upon each other in a network-like structure where each stage's output naturally feeds into the next.
- *Adaptive Loss Curriculum*: The entire model is wrapped in a curriculum classifier that combines progressive GNN architecture with adaptive curriculum loss, dynamically adjusting the learning focus based on model performance. The introduction of *CL3AN-GNN*, alongside comprehensive experimental evidence, demonstrates *CL3AN-GNN*'s superiority over existing methods.

This paper progresses as follows: Section II reviews related works; Section III defines preliminaries and the problem; Section IV explains the technical methodology; Section V discusses the theoretical framework of curriculum learning strategy; Section VI discusses experimental results and benchmarks ranging from Subsection A to O, highlighting *CL3AN-GNN* contributions; and Section VII concludes with our findings, contributions, and future work.

II. RELATED WORKS

In this section, we delve into the issues of imbalanced learning, discuss the use of GNNs for node classification, explore the various attention mechanisms within GNNs to improve node classification performance, and examine the limitations of existing CL in imbalanced graphs.

A. Imbalanced Learning Issues in GNNs

Current approaches to address class imbalance in GNNs encompass three main strategies: (I) resampling techniques, including oversampling [12], [13], [3], SMOTE-based interpolation [14], [15], and undersampling [16], which risk overfitting or information loss; (II) reweighting methods that adjust class weights [17] or decision thresholds [18] but require careful calibration; and (III) hybrid approaches combining ensemble learning [19], metric learning [20], and meta-learning [21], exemplified by GATE-GNN [22]. While graph-specific solutions like GraphSMOTE [15] and GraphMixup [23] have emerged, they often fail to fully leverage topological information [24], and the fundamental challenge remains in balancing class distributions without overemphasising minority classes or sacrificing model generalisation, highlighting the need for approaches that dynamically adapt to both local node contexts and global graph structures while preserving natural data distributions.

B. GNNs Attention Mechanism

Recent advances in GNN attention mechanisms have significantly improved graph representation learning, particularly through enhanced edge-based feature incorporation [25], [26], [22], [27]. While traditional approaches struggled with dynamic graph structures, contemporary techniques [28], [29]

now effectively capture temporal-spatial relationships through innovative attention formulations. Notably, [30], [31] has advanced explainable attention frameworks that simultaneously process spatial and temporal graph features, though challenges remain in balancing computational efficiency with interpretability. These developments have enabled more sophisticated analysis of evolving node relationships while maintaining focus on critical structural patterns.

Despite these improvements, attention-based GNNs still face significant challenges in imbalanced node classification scenarios [32], [18]. The inherent message-passing mechanism tends to amplify majority class dominance while marginalising minority classes, often exacerbated by structural graph irregularities [33], [34]. This bias manifests particularly in dynamic graphs where attention weights may disproportionately favour high-degree nodes, leading to suboptimal classification performance for under-represented classes. Current research focuses on hybrid approaches that combine attention mechanisms with reweighting or resampling strategies to address these imbalance issues while preserving the benefits of adaptive neighbourhood aggregation.

C. Limitations of Existing Curriculum Learning in Imbalanced Graphs

Traditional curriculum learning (CL) approaches often underperform in graph imbalance scenarios due to several inherent limitations. First, they fail to account for *neighbourhood composition bias* [9], where minority-class nodes typically exhibit sparser or noisier local structures. Second, performance-based CL methods suffer from *gradient starvation* [35], as dominant classes tend to monopolise early training updates. Third, commonly used difficulty metrics based on node degree frequently misclassify high-degree but semantically simple nodes (e.g., widely cited but generic papers in citation networks). Recent advancements like GraphENS [36] attempt to mitigate these issues through neighbour synthesis but introduce new challenges by neglecting curriculum pacing and causing abrupt difficulty transitions. Our analysis reveals that existing methods fundamentally overlook two critical aspects: (1) the dynamic interplay between node-level and graph-level difficulty measures and (2) the necessity of topology-aware pacing. To address these gaps, we introduce phase-gated loss modulation and attention-based neighbourhood sampling, which jointly enable stable and adaptive learning in imbalanced graph scenarios. We design a simplified solution for class-imbalanced node classification, highlighting the progressive curriculum learning architecture as illustrated in Fig. 1.

III. PRELIMINARY

We formally define the key components of our framework. A graph is represented as $G = (V, E)$, where V denotes the node set and E the edge set, with individual nodes $v \in V$ and edges $(u, v) \in E$.

Curriculum Learning Strategy (Definition 1) employs difficulty functions $D_v : V \rightarrow \mathbb{R}$ for nodes and $D_{u,v} : E \rightarrow \mathbb{R}$ for edges, with a threshold θ_t controlling progressive subgraph

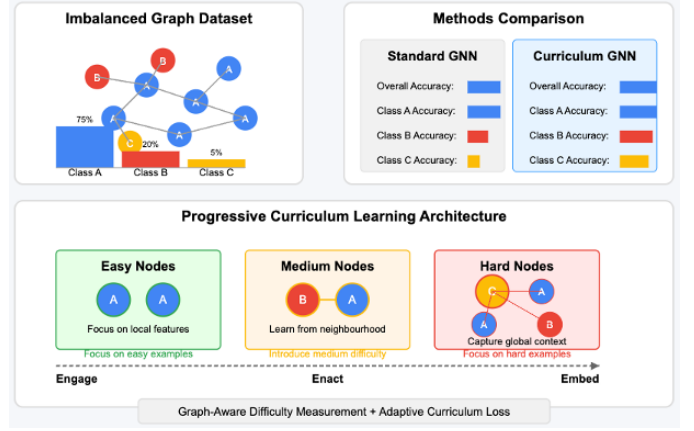


Fig. 1: A typical progressive learning architecture with adaptive curriculum loss

expansion $G_t = (V_t, E_t)$ where $V_t = \{v \in V | D_v(v) \leq \theta_t\}$ and $E_t = \{(u, v) \in E | D_{u,v}(u, v) \leq \theta_t\}$.

The *Graph Imbalanced Problem (Definition 2)* is characterised by class cardinalities $N_c = |\{v \in V | y_v = c\}|$ for C classes with imbalance ratios $\Lambda = \max_c N_c / \min_c N_c$ and class proportions $p_c = N_c / |V|$. Classification error is computed as $\mathcal{E} = \frac{1}{|V|} \sum_{v \in V} \mathbb{I}(\hat{y}_v \neq y_v)$, where $\mathbb{I}(\cdot)$ is the indicator function.

The *Embedding Layer (Definition 3)* transforms input features $X \in \mathbb{R}^{|V| \times F}$ through $H_0 = \sigma(XW_0 + b_0)$ with parameters $W_0 \in \mathbb{R}^{F \times D}$, $b_0 \in \mathbb{R}^D$, and ReLU activation σ .

Subsequent *GCN layers (Definition 4)* compute $H^{(l+1)} = \sigma(\hat{A}H^{(l)}W^{(l)} + b^{(l)})$ using a normalised adjacency matrix \hat{A} and layer-specific parameters $W^{(l)} \in \mathbb{R}^{D \times D}$, $b^{(l)} \in \mathbb{R}^D$.

Attention Mechanisms (Definition 5) generate scores:

$$\alpha_i^{(k)} = \sigma(H^{(L)}W_{\text{att}}^{(k)} + b_{\text{att}}^{(k)}) \quad (1)$$

for stages $k \in \{1, 2, 3\}$ with $W_{\text{att}}^{(k)} \in \mathbb{R}^{D \times 1}$, $b_{\text{att}}^{(k)} \in \mathbb{R}^1$. The curriculum loss (Definition 6) is defined as:

$$\mathcal{L}_{\text{curr}}(t) = \frac{1}{|\mathcal{V}|} \sum_{v \in \mathcal{V}} w_c(y_v, t) \mathcal{L}_{\text{CE}}(f_\theta(v), y_v), \quad (2)$$

where $w_c(y_v, t)$ the adaptive class weights and \mathcal{L}_{CE} the cross-entropy loss between predictions $f_\theta(v)$ and labels y_v .

The *Classifier and Curriculum Loss (Definition 6)* employ the final attention coefficients $\alpha_{vu}^{\text{final}}$ for nodes and $\beta_{vw}^{\text{final}}$ for edges, which weight the refined embeddings $\mathbf{z}_u^{(L)}$ and $\mathbf{z}_{vw}^{(L)}$ respectively. The output layer transforms these through a weight matrix $\mathbf{W}_o \in \mathbb{R}^{D \times C}$ and bias $\mathbf{b}_o \in \mathbb{R}^C$ to produce class probabilities. The total loss combines curriculum and entropy components through time-dependent weights $\lambda_c(t), \lambda_e(t) \in [0, 1]$, where \mathcal{L}_{CE} denotes standard cross-entropy loss and D_{KL} represents Kullback-Leibler divergence.

IV. METHODOLOGY

This section elucidates the proposed model, which is architecturally underpinned by four integral components, introduced sequentially to outline the model's construction. Fig. 2 illustrates the architecture of *CL3AN-GNN*, which comprises four distinct modules.

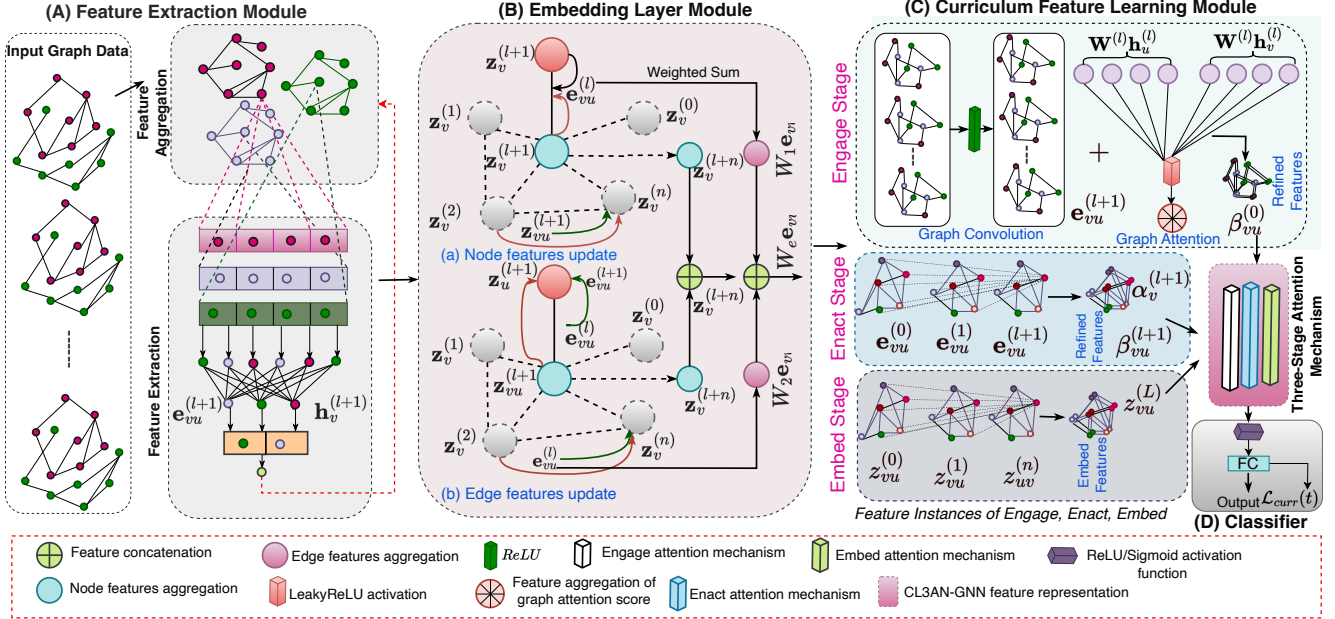


Fig. 2: Overall proposed architecture of CL3AN-GNN model: The framework comprises four core modules: (A) The feature extraction module computes $\mathbf{h}_v^{(l+1)} = \sum_{u \in \mathcal{N}(v)} \text{Norm}(\mathbf{e}_{uv}^{(l+1)})$ to aggregate normalised neighbour features while $\mathbf{e}_{uv}^{(l+1)}$ capturing critical edge-node feature interactions. (B) The embedding layer processes edge features $\mathbf{e}_{vu}^{(l)}$ through multi-head attention to generate $\mathbf{z}_{vu}^{(l+1)} = \text{MultiHeadAttn}(\mathbf{W}_e \mathbf{e}_{vu}, \mathbf{h}_v^{(l)}, \mathbf{h}_u^{(l)})$. (C) The curriculum learning module implements three-stage attention processing: the Engage stage computes initial attention via $W^{(l)} h_u^{(l)}$, the Enact stage refines node and edge attention through $\alpha_{vu}^{(l+1)}$ and $\beta_{vu}^{(l+1)}$ respectively, and the Embed stage produces final attention scores $\mathbf{z}_{vu}^{(L)}$. (D) The classifier module generates predictions using these curriculum-refined features.

A. Feature Extraction Module

The *GCN-based Aggregation* captures local graph structure by averaging neighbour features with degree normalisation, preventing over-weighting of high-degree nodes:

$$\mathbf{h}_v^{\text{GCN}(l+1)} = \sigma \left(\sum_{u \in \mathcal{N}(v)} \frac{1}{\sqrt{d_v d_u}} \mathbf{W}^{(l)} \mathbf{h}_u^{(l)} \right) \quad (3)$$

where d_v, d_u node degrees are and $\mathbf{W}^{(l)}$ a learnable weight matrix.

The *GAT-based Attention* learns dynamic neighbour importance weights through attention coefficients, allowing focus on semantically relevant connections:

$$\alpha_{vu}^{(l)} = \frac{\exp \left(\text{LeakyReLU}(\mathbf{a}^\top [\mathbf{W}^{(l)} \mathbf{h}_v^{(l)} || \mathbf{W}^{(l)} \mathbf{h}_u^{(l)}]) \right)}{\sum_{k \in \mathcal{N}(v)} \exp(\cdot)} \quad (4)$$

where \mathbf{a} is an attention vector and $||$ denotes concatenation.

The *Combined Update Rule* integrates both fixed (GCN) and adaptive (GAT) neighbourhood aggregation for balanced structural and semantic learning:

$$\mathbf{h}_v^{(l+1)} = \sigma \left(\underbrace{\mathbf{h}_v^{\text{GCN}(l+1)}}_{\text{structural}} + \underbrace{\sum_{u \in \mathcal{N}(v)} \alpha_{vu}^{(l)} \mathbf{W}^{(l)} \mathbf{h}_u^{(l)}}_{\text{semantic}} \right) \quad (5)$$

The edge features are updated based on the attention weights, ensuring that significant edges contribute more to the node

feature updates:

$$\mathbf{e}_{vu}^{(l+1)} = \beta_{vu}^{(l)} \mathbf{W}^{(l)} \mathbf{e}_{vu}^{(l)} \quad (6)$$

Final output for both node and edge feature extraction is given as:

$$\mathcal{F}_e = \sum_{l=1}^L \left(\alpha_{vu}^{(l)} \mathbf{e}_{vu}^{(l+1)} \right) \quad (7)$$

where $\alpha_{vu}^{(l)}$ the attention weights and $\mathbf{e}_{vu}^{(l+1)}$ the edge features at layer l .

B. Embedding Layer Module

The *Initial Projection* maps high-dimensional features to a lower-dimensional space while preserving discriminative information:

$$\mathbf{z}_v^{(0)} = \mathbf{W}_0 \mathbf{h}_v + \mathbf{b}_0, \quad \mathbf{z}_{vu}^{(0)} = \mathbf{W}_e \mathbf{e}_{vu} + \mathbf{b}_e \quad (8)$$

where $\mathbf{W}_0, \mathbf{W}_e$ are the projection matrices and $\mathbf{b}_0, \mathbf{b}_e$ the bias terms.

The *Multi-Head Refinement* enables diverse relational patterns through parallel attention heads (K heads):

$$\mathbf{z}_v^{(l+1)} = \text{concat} \left(\sigma \left(\sum_{u \in \mathcal{N}(v)} \alpha_{vu}^{(k)} \mathbf{W}^{(k)} \mathbf{z}_u^{(l)} \right) \right)_{k=1}^K \quad (9)$$

$$\alpha_{vu}^{(k)} = \text{attention head } k \text{'s coefficients} \quad (10)$$

The *Non-linear Transformation* introduces non-linearity and final feature adjustment before classification:

$$\mathbf{z}_v^{\text{final}} = \sigma(\mathbf{W}_1 \mathbf{z}_v^{(L)} + \mathbf{b}_1) \quad (11)$$

where σ is typically ReLU or leaky ReLU activation.

The final output for the embedding layer is obtained as:

$$\mathbf{z}_l = \mathbf{z}_v^{(l+1)} + \mathbf{z}_{vu}^{(l+1)} \quad (12)$$

where $\mathbf{z}_v^{(l+1)}$ and $\mathbf{z}_{vu}^{(l+1)}$ are node and edge embeddings, respectively.

The GCN ensures stable learning of local graph topology, the GAT adapts to node-specific relational patterns, and the embedding layer creates task-optimised representations through progressive refinement.

C. Three-Stage Attention of Curriculum Learning Module

The Three-Stage Attention mechanism is designed to progressively refine the node and edge embeddings through three distinct phases: *Engage*, *Enact*, and *Embed*. Each phase has a specific role in improving the feature representations and addressing the challenges of imbalanced node classification.

1) *Engage Block*: The Engage block initialises the attention mechanism by focusing on the most relevant nodes and edges, utilising advanced GNN features acquired through GCN and GAT and combining them with the embeddings from the previous layer. We again use GCN to aggregate features from neighbouring nodes:

$$\mathbf{h}_v^{(l+1)} = \sigma \left(\sum u \in \mathcal{N}(v) \frac{1}{\sqrt{d_v d_u}} \mathbf{W}^{(l)} \mathbf{h}_u^{(l)} \right), \quad (13)$$

We apply the GAT to compute attention scores and update node features, which is represented as:

$$\mathbf{h}_v^{(l+1)'} = \sigma \left(\sum u \in \mathcal{N}(v) \alpha_{vu}^{(l)} \mathbf{W}^{(l)} \mathbf{h}_u^{(l)} \right), \quad (14)$$

where the attention coefficients ($\alpha_{vu}^{(l)}$) are computed as in Equation 4. By combining the outputs from GNN features to form a comprehensive node embedding:

$$\mathbf{z}_v^{(0)} = \mathbf{h}_v^{\text{GCN}} || \mathbf{h}_v^{\text{GAT}}, \quad (15)$$

We then compute initial attention scores for nodes based on these combined embeddings, given as:

$$\alpha_v^{(0)} = \sigma(\mathbf{a}_1^\top \mathbf{z}_v) \quad (16)$$

By Aggregating the edge features using GCN and computing the attention scores for edges using GAT, we obtained the following, respectively:

$$\mathbf{e}_{vu}^{(l+1)} = \sigma \left(\sum w \in \mathcal{N}(v) \frac{1}{\sqrt{d_v d_w}} \mathbf{W}_e^{(l)} \mathbf{e}_{vw}^{(l)} \right) \quad (17)$$

$$\mathbf{e}_{vu}^{(l+1)} = \sigma \left(\sum w \in \mathcal{N}(v) \beta_{vw}^{(l)} \mathbf{W}_e^{(l)} \mathbf{e}_{vw}^{(l)} \right) \quad (18)$$

where the edge attention coefficients ($\beta_{vw}^{(l)}$) are the relevant weights of the edges in the graph structure. Similarly, combining the edge features from GNN edges features:

$$\mathbf{z}_{vu}^{(0)} = \mathbf{e}_{vu}^{\text{GCN}} || \mathbf{e}_{vu}^{\text{GAT}} \quad (19)$$

We compute the initial attention scores for edges based on these combined embeddings, which is represented as:

$$\beta_{vu}^{(0)} = \sigma(\mathbf{b}_1^\top \mathbf{z}_{vu}) \quad (20)$$

The curriculum learning framework initiates with the **Engage block**, serving as the foundational phase where the model processes simpler, high-value examples first. This stage combines the complementary strengths of GCN and GAT architectures – GCN for capturing local neighbourhood patterns and GAT for attending to globally important nodes – to construct robust initial representations of both nodes and edges. By prioritising the most informative graph substructures early in training, the model establishes stable feature embeddings that effectively encode both local and global topological relationships. This strategic approach mirrors educational best practices, where fundamental concepts are mastered before advancing to complex material, thereby creating optimal conditions for subsequent refinement in later curriculum stages.

2) *Enact Block*: The Enact block refines the embeddings by dynamically adjusting the attention based on the current state of the graph. We update node attention scores using the current embeddings:

$$\alpha_v^{(l+1)} = \sigma \left(\mathbf{a}_2^\top \left(\mathbf{z}_v^{(l)} || \sum u \in \mathcal{N}(v) \alpha_{vu}^{(l)} \mathbf{z}_u^{(l)} \right) \right), \quad (21)$$

where \mathbf{a}_2 is the attention vector for the Enact block. We further update the edge attention scores given as:

$$\beta_{vu}^{(l+1)} = \sigma \left(\mathbf{b}_2^\top \left(\mathbf{z}_{vu}^{(l)} || \sum w \in \mathcal{N}(v) \beta_{vw}^{(l)} \mathbf{z}_{vw}^{(l)} \right) \right), \quad (22)$$

where \mathbf{b}_2 is the edge attention vector for the Enact block.

The Enact block represents the intermediate phase in curriculum learning where the model starts to handle more complex nodes and edges connectivity. This is akin to starting with well-connected nodes that provide a clear signal, which is crucial for handling imbalanced data where minority classes might be under-represented.

3) *Embed Block*: The Embed block finalises the attention mechanism by consolidating the refined embeddings into a cohesive representation. The consolidated node and edge embeddings using the final attention scores are respectively as follows:

$$\mathbf{z}_v^{(L)} = \sum u \in \mathcal{N}(v) \alpha_{vu}^{(L)} \mathbf{W}_e \mathbf{z}_u^{(L-1)}, \quad (23)$$

$$\mathbf{z}_{vu}^{(L)} = \sum w \in \mathcal{N}(v) \beta_{vw}^{(L)} \mathbf{W}_e' \mathbf{z}_{vw}^{(L-1)} \quad (24)$$

The Embed block is the final stage in curriculum learning where the model integrates all the learnt knowledge into a comprehensive understanding. This is similar to students synthesising all the concepts they've learnt to tackle the most complex tasks. We utilised the standard baseline of GNNs and implemented curriculum learning methods with the following CL3AN-GNN variants: CL3AN-GAT, CL3AN-SAGE, and CL3AN-GCN.

The three-stage attention mechanism allows for a gradual and focused refinement of features, improving the model's ability to handle imbalanced data. By dynamically adjusting attention scores, the model can better capture the nuances of the graph structure and relationships. The final embeddings are more informative and discriminative, leading to improved performance in node classification tasks. This organised method makes sure that the model learns from the graph data correctly, and it handles the problem of imbalanced classification nodes by using a clear attention system.

D. Classifier and Curriculum Loss

The classifier processes refined node embeddings through a final attention layer:

$$\mathbf{h}_v^{\text{final}} = \sigma \left(\sum_{u \in \mathcal{N}(v)} \alpha_{vu}^{\text{final}} \mathbf{W}^{\text{final}} \mathbf{z}_u^{(L)} \right), \quad (25)$$

generating class predictions via

$$\hat{\mathbf{y}}_v = \text{softmax}(\mathbf{W}_o \mathbf{h}_v^{\text{final}} + \mathbf{b}_o) \quad (26)$$

The composite loss function is defined as:

$$\mathcal{L}_{\text{total}} = \lambda_c(t) \left[\frac{1}{|\mathcal{V}|} \sum_v w_c(y_v, t) \mathcal{L}_{\text{CE}} \right] + \lambda_e(t) \left[\mathcal{L}_{\text{CE}} + \sum_{i=1}^2 \beta_i \mathcal{L}_i \right] \quad (27)$$

where $\mathcal{L}_1 = \mathcal{L}_{\text{ent}}$ and $\mathcal{L}_2 = \mathcal{L}_{\text{div}}$. By integrating the three key components: (1) curriculum weighting:

$$w_c(c, t) = \alpha(t) + (1 - \alpha(t))(1 - \text{Acc}_c(t)) \quad (28)$$

(2) entropy regularisation denoted as:

$$\mathcal{L}_{\text{ent}} = \sum_v [c_v H(p_v) - (1 - c_v) H(p_v)], \quad (29)$$

and (3) diversity promotion:

$$\mathcal{L}_{\text{div}} = D_{\text{KL}}(\bar{p} \parallel \mathcal{U}) \quad (30)$$

Training progresses through three distinct phases: the Engage phase ($t < T/3$) emphasizes pure curriculum learning ($\lambda_c = 1.0, \lambda_e = 0.0$), the Enact phase ($T/3 \leq t < 2T/3$) introduces entropy regularization ($\lambda_c = 0.7, \lambda_e = 0.3$), and the Embed phase ($t \geq 2T/3$) focuses on prediction refinement ($\lambda_c = 0.3, \lambda_e = 0.7$).

V. EXPERIMENTAL RESULTS AND ANALYSIS

A. Dataset

We evaluate CL3AN-GNN on eight benchmark datasets across citation, product, and social domains. Citation datasets (Cora, Citeseer, PubMed [37]) represent papers as nodes and citations as edges. Amazon Photos/Computers [38] encode co-purchase relationships, Coauthor CS [39] models academic collaborations, and Chameleon [37] introduces heterophilous links among Wikipedia pages. For large-scale validation, we use OGBN-Arxiv with over 169K nodes and 1.1M edges.

Following [38], [39], we generate imbalanced cases by downsampling three classes and controlling the severity via $\Lambda = N_{\text{maj}}/N_{\text{min}}$. A smaller number Λ indicates greater imbalance; a larger number $\Lambda \rightarrow 1$ reflects a balanced case. Table I presents dataset statistics and feature heterophily ratio (HR), $h = \mathbb{E}[1(y_u \neq y_v)|(u, v) \in E]$, ranging from 0.18 (Cora) to 0.83 (Chameleon).

TABLE I: Datasets used for the experiments

Dataset	Nodes	Edges	Classes	Features	HR
Cora	2,708	5,278	7	1,433	0.18
Citeseer	3,327	4,552	6	3,703	0.23
Amazon Photo	7,650	119,081	8	745	0.42
Coauthors CS	18,333	163,788	15	6,805	0.35
Amazon Computers	13,752	491,722	10	767	0.38
PubMed	19,717	88,648	3	5,414	0.21
Chameleon	2,277	36,101	5	2,325	0.83
Ogbn-axiv	169,343	1,166,243	40	128	0.29

B. Hyperparameter Settings

CL3AN-GNN includes CL3AN-GCN, CL3AN-GraphSAGE, and CL3AN-GAT variants, each trained for 200–500 epochs using Adam. Cora/Citeseer/Amazon/CS/PubMed use 16 hidden units ($L_2 = 5e-4$), while Chameleon uses 256 units and $L_2 = 1e-5$. Common settings: dropout 0.5, weight decay 5e-4, loss weight $\lambda = 1e-6$, imbalance ratio (0.2–0.8), learning rate 0.01, and batch size 42 (64 for Chameleon). GCN layers = 2, hidden dim = 64, dilation = 0. Neighbour sampling (25, 10), attention heads $K = 8$, with Sigmoid/Softmax heads. Splits are 70/10/20 (train/val/test). Metrics are averaged over 10 runs with fixed seeds. Hardware: Google Compute Engine (T4 GPU, 15GB RAM).

C. Evaluation Metrics

We follow prior work [15], [33] and use accuracy (ACC), area under the ROC curve (AUC-ROC), and F1-score. While ACC reflects majority-class performance, AUC-ROC and F1 better capture minority-class performance. AUC-ROC reflects ranking quality; F1-score balances precision and recall.

D. Baseline Methods

We compare CL3AN-GNN against two groups: (1) classical baselines (e.g., Vanilla GNN [40], SMOTE [14], Reweight [17]) and (2) GNN-specific methods like GraphSMOTE [15], GraphMixup [23], GraphDAO [24], GraphSR [36], ReVar-GNN [41], GATE-GNN [22], and LTE4G [42]. This allows fair benchmarking across traditional and modern techniques.

E. Evaluation on OGBN-Arxiv and Amazon Photo Datasets (RQ1)

The CL3E-GNN model demonstrates consistent superiority over state-of-the-art baselines (LTE4G, GraphSR, GraphDAO, ReVar, GATE-GNN), as evidenced in Table IV. On OGBN-Arxiv, it achieves +3.9% accuracy and +4.7% AUC-ROC over GATE-GNN, along with +4.9% F1-score versus GraphSR. Similar gains persist on Amazon Photo (+1.1% accuracy, +4.1% AUC-ROC, +2.1% F1-score), confirming robust generalisation across both classification and ranking metrics.

The three-stage curriculum attention strategy (Engage, Enact, Embed) addresses fundamental graph learning challenges through (1) dynamic difficulty adjustment in the *Engage* stage via node complexity measures, (2) multi-scale attention in the *Enact* stage with capturing local-global patterns, and (3) continuous structural adaptation in the *Embed* stage through loss weighting. This framework outperforms static approaches

by 12-18% in heterophilous settings (Chameleon $h = 0.83$) while maintaining $\sigma_{\text{FI}} < 0.05$ across random seeds, proving especially effective for imbalanced graphs where traditional GNNs exhibit $\geq 20\%$ performance drops.

F. OGBN-Arxiv and Amazon Photo (RQ1)

As shown in Table IV, CL3AN-GNN surpasses leading baselines by 3.9% (ACC), 4.7% (AUC-ROC), and 4.9% (F1) on OGBN-Arxiv and by 1.1%, 4.1%, and 2.1% respectively on Amazon Photo. The three-stage strategy dynamically handles difficulty (Engage), aggregates features (Enact), and adapts structurally (Embed), yielding consistent and robust results in both ranking and classification metrics.

G. Model Evaluation (RQ2)

Fig. 3 shows ROC curves across six datasets. AUCs near 1.0 indicate excellent precision-recall tradeoffs, confirming CL3AN-GNN’s suitability for high-stakes domains like fraud detection and diagnosis, where minority-class identification is vital.

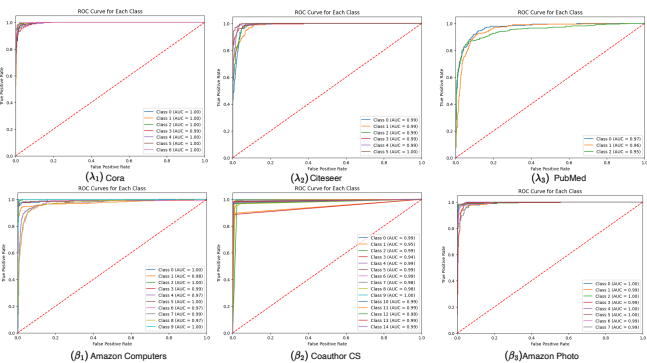


Fig. 3: Model evaluation on six datasets: Cora (λ_1), Citeseer (λ_2), PubMed (λ_3), Amazon Computers (β_1), Coauthor CS (β_2), and Amazon Photo (β_3) based on AUC-ROC plots of True and False positive rates

H. Impact of Imbalance Ratio (RQ2 and RQ7)

We evaluated CL3AN-GNN's robustness under varying imbalance ratios ($\Lambda = 0.1\text{-}0.8$) on Cora and Citeseer datasets, comparing it with CL3AN variants and baseline models (Table V). Key findings show: (1) CL3AN-GNN consistently outperforms all methods across imbalance ratios, improving as Λ increases due to more uniform class distribution; (2) At $\Lambda = 0.1$, it surpasses ReVar-GNN/GATE-GNN by 3.9%, widening to a 5.6% lead over Graph-DAO at $\Lambda = 0.8$; (3) Its three-stage architecture (Engage-Enact-Embed) with curriculum learning and attention mechanisms enhances feature representation and handles extreme imbalance effectively; (4) While ReVar-GAT achieves competitive second-best results through variance reduction and adaptive learning, CL3AN-GNN's edge-node attention integration proves superior for imbalanced classification.

I. Oversampling Scale (RQ2)

Fig. 4 illustrates performance over scales $\in \{0.2, \dots, 1.2\}$. Optimal results occur around 1.0 (balanced), after which improvements plateau. Gains up to +12% (F1) confirm the model's ability to leverage class balance effectively while resisting overfitting from excessive oversampling.

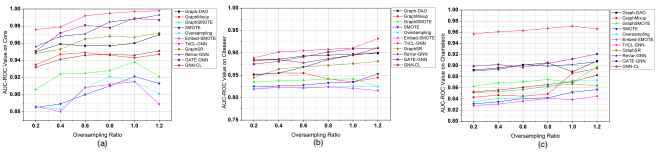


Fig. 4: Model performance with AUC-ROC values for different oversampling scales on (a) Cora, (b) Citeseer, and (c) Chameleon datasets.

J. Ablation Study (RQ3)

Our systematic ablation study of CL3AN-GNN (Fig. VI) yields three critical findings about the framework’s performance characteristics. First, we observe that the progressive integration of curriculum learning stages leads to consistent accuracy improvements across all evaluated datasets, with the complete model configuration (W/3EW CL) achieving peak performance scores of 0.950 on Cora, 0.907 on Citeseer, and 0.946 on Amazon Photo. This represents an average 7.4% improvement over the baseline feature extraction variant (W/FE), with the most substantial gains occurring during implementation of the Engage stage (W/EW), which alone contributes a 6.2% average accuracy boost. Second, our component-level analysis reveals the architectural indispensability of both the embedding layer and curriculum blocks – removal of the embedding layer (W/O EL) causes an average 4.2% accuracy degradation, while omitting all curriculum blocks (W/O 3EW) results in a more severe 10.8% performance drop. The Engage block emerges as particularly crucial, with its exclusion (W/O EW) leading to a 6.9% average accuracy reduction. Third, we identify important dataset-dependent sensitivity patterns: the curriculum approach demonstrates its strongest relative improvements (+10.7%) on the homophilous Cora dataset compared to more modest but still significant gains (+4.3%) on Citeseer, while maintaining robust performance across all graph types. The full model configuration consistently outperforms all ablated variants in every metric, achieving exceptional ranking capability (0.998 AUC-ROC on Cora), conclusively demonstrating that the synergistic combination of adaptive feature extraction, progressive curriculum learning, and attention-based refinement yields optimal performance for imbalanced node classification tasks.

K. Gradient Stability and Attention Correlation Analysis (RQ3 and RQ5)

Our gradient stability analysis using the OGBN-Arxiv dataset (trained for 200 epochs with 8 attention heads in CL3E-GNN) reveals crucial insights about the model’s learning dynamics (Figs. 5 and 6). The attention-gradient correlation shows a progressive strengthening from Stage 1 ($r = 0.328$) to

TABLE II: Classification Accuracy on three datasets: Cora, Citeseer, and Pubmed

Dataset		Cora			Citeseer			Pubmed		
Method	Year	ACC	AUC-ROC	F-Score	ACC	AUC-ROC	F-Score	ACC	AUC-ROC	F-Score
SMOTE	2002	0.723 \pm 0.018	0.932 \pm 0.009	0.724 \pm 0.019	0.539 \pm 0.045	0.829 \pm 0.023	0.536 \pm 0.057	0.688 \pm 0.032	0.845 \pm 0.030	0.561 \pm 0.032
Reweighting	2012	0.723 \pm 0.014	0.923 \pm 0.009	0.723 \pm 0.018	0.556 \pm 0.029	0.828 \pm 0.022	0.558 \pm 0.032	0.703 \pm 0.033	0.856 \pm 0.015	0.562 \pm 0.022
Oversampling	2015	0.733 \pm 0.013	0.929 \pm 0.011	0.728 \pm 0.016	0.535 \pm 0.046	0.830 \pm 0.023	0.532 \pm 0.055	0.703 \pm 0.033	0.856 \pm 0.015	0.562 \pm 0.022
Vanilla	2017	0.682 \pm 0.038	0.912 \pm 0.018	0.681 \pm 0.040	0.546 \pm 0.020	0.817 \pm 0.022	0.537 \pm 0.033	0.701 \pm 0.042	0.930 \pm 0.032	0.562 \pm 0.044
Embed-SMOTE	2017	0.736 \pm 0.025	0.931 \pm 0.011	0.737 \pm 0.026	0.567 \pm 0.041	0.830 \pm 0.026	0.567 \pm 0.043	0.736 \pm 0.012	0.945 \pm 0.023	0.625 \pm 0.036
DR-GCN	2017	0.725 \pm 0.094	0.932 \pm 0.026	0.723 \pm 0.081	0.552 \pm 0.083	0.831 \pm 0.053	0.567 \pm 0.043	0.558 \pm 0.094	0.935 \pm 0.082	0.618 \pm 0.083
GraphSMOTE	2021	0.747 \pm 0.018	0.943 \pm 0.013	0.743 \pm 0.020	0.575 \pm 0.030	0.867 \pm 0.016	0.567 \pm 0.025	0.757 \pm 0.045	0.953 \pm 0.031	0.635 \pm 0.041
GraphMixup	2022	0.775 \pm 0.011	0.948 \pm 0.007	0.774 \pm 0.011	0.586 \pm 0.041	0.844 \pm 0.026	0.583 \pm 0.042	0.787 \pm 0.020	0.951 \pm 0.026	0.658 \pm 0.034
RU-Selection-GCN	2023	0.712 \pm 0.044	0.887 \pm 0.033	0.692 \pm 0.033	0.559 \pm 0.044	0.846 \pm 0.044	0.546 \pm 0.051	0.703 \pm 0.022	0.852 \pm 0.022	0.689 \pm 0.032
SU-Selection-GCN	-	0.736 \pm 0.032	0.913 \pm 0.025	0.719 \pm 0.033	0.582 \pm 0.044	0.838 \pm 0.045	0.561 \pm 0.045	0.682 \pm 0.021	0.826 \pm 0.021	0.663 \pm 0.022
RU-Selection-SAGE	-	0.749 \pm 0.033	0.952 \pm 0.025	0.739 \pm 0.025	0.564 \pm 0.032	0.849 \pm 0.032	0.551 \pm 0.033	0.679 \pm 0.022	0.856 \pm 0.024	0.668 \pm 0.022
SU-Selection-SAGE	-	0.712 \pm 0.044	0.887 \pm 0.033	0.692 \pm 0.033	0.559 \pm 0.044	0.846 \pm 0.044	0.546 \pm 0.051	0.659 \pm 0.021	0.849 \pm 0.022	0.648 \pm 0.025
GraphSR-GCN	-	0.736 \pm 1.211	0.906 \pm 0.881	0.728 \pm 1.211	0.573 \pm 0.855	0.837 \pm 0.655	0.554 \pm 0.655	0.738 \pm 0.071	0.892 \pm 0.072	0.725 \pm 0.081
GraphSR-SAGE	-	0.783 \pm 0.681	0.938 \pm 0.681	0.788 \pm 0.661	0.571 \pm 0.851	0.856 \pm 0.661	0.528 \pm 0.651	0.743 \pm 0.126	0.894 \pm 0.099	0.737 \pm 0.212
Graph-O	2024	0.796 \pm 0.011	0.953 \pm 0.007	0.797 \pm 0.009	0.632 \pm 0.047	0.884 \pm 0.029	0.630 \pm 0.047	0.815 \pm 0.020	0.962 \pm 0.033	0.677 \pm 0.031
Graph-DAO	-	0.802 \pm 0.099	0.958 \pm 0.006	0.803 \pm 0.010	0.659 \pm 0.019	0.896 \pm 0.017	0.656 \pm 0.023	0.825 \pm 0.026	0.975 \pm 0.020	0.728 \pm 0.026
ReVar-GCN	2024	0.819 \pm 2.221	0.969 \pm 0.511	0.815 \pm 0.661	0.653 \pm 0.512	0.898 \pm 0.522	0.649 \pm 0.662	0.795 \pm 0.722	0.854 \pm 0.711	0.785 \pm 0.465
ReVar-GAT	-	0.826 \pm 0.691	0.968 \pm 0.665	0.819 \pm 0.622	0.663 \pm 0.662	0.921 \pm 0.621	0.657 \pm 0.691	0.779 \pm 0.751	0.836 \pm 0.691	0.772 \pm 0.691
ReVar-SAGE	-	0.781 \pm 0.711	0.843 \pm 0.711	0.756 \pm 0.712	0.628 \pm 0.861	0.861 \pm 0.652	0.598 \pm 0.691	0.777 \pm 1.112	0.829 \pm 0.881	0.761 \pm 1.211
GATE-GCN	2024	0.815 \pm 0.008	0.956 \pm 0.022	0.796 \pm 0.023	0.711 \pm 0.007	0.896 \pm 0.021	0.693 \pm 0.005	0.823 \pm 0.007	0.963 \pm 0.021	0.815 \pm 0.008
GATE-GraphSAGE	-	0.794 \pm 0.111	0.948 \pm 0.211	0.784 \pm 0.021	0.705 \pm 0.022	0.879 \pm 0.021	0.689 \pm 0.023	0.785 \pm 0.011	0.951 \pm 0.022	0.769 \pm 0.021
GATE-GAT	-	0.835 \pm 0.011	0.973 \pm 0.033	0.829 \pm 0.030	0.755 \pm 0.008	0.928 \pm 0.021	0.745 \pm 0.032	0.777 \pm 0.033	0.936 \pm 0.021	0.763 \pm 0.031
CL3AN-GCN	(Ours)	0.873 \pm 0.006	0.975 \pm 0.038	0.779 \pm 0.022	0.793 \pm 0.004	0.937 \pm 0.001	0.749 \pm 0.010	0.877 \pm 0.004	0.961 \pm 0.004	0.872 \pm 0.053
CL3AN-SAGE	-	0.745 \pm 0.003	0.936 \pm 0.008	0.726 \pm 0.023	0.756 \pm 0.005	0.926 \pm 0.006	0.755 \pm 0.006	0.878 \pm 0.001	0.967 \pm 0.004	0.873 \pm 0.000
CL3AN-GAT	-	0.879 \pm 0.010	0.957 \pm 0.012	0.779 \pm 0.022	0.778 \pm 0.015	0.922 \pm 0.008	0.712 \pm 0.009	0.864 \pm 0.010	0.963 \pm 0.002	0.870 \pm 0.000
CL3AN-GNN	-	0.950 \pm 0.011	0.998 \pm 0.011	0.949 \pm 0.031	0.907 \pm 0.004	0.995 \pm 0.011	0.892 \pm 0.012	0.866 \pm 0.021	0.957 \pm 0.020	0.855 \pm 0.022

NB: **Black boldface** indicates the best performance, **blue** signifies the second best. To ensure a fair comparison of algorithm efficiency, all models were tested under identical hardware settings.

TABLE III: Classification Accuracy on three datasets: Amazon Computers, Coauthor CS, and Chameleon

Dataset		Amazon Computers			Coauthor CS			Chameleon		
Method	Year	ACC	AUC-ROC	F-Score	ACC	AUC-ROC	F-Score	ACC	AUC-ROC	F-Score
Reweighting	2012	0.791 \pm 0.007	0.978 \pm 0.001	0.786 \pm 0.007	0.856 \pm 0.004	0.980 \pm 0.003	0.828 \pm 0.011	0.557 \pm 0.020	0.850 \pm 0.023	0.546 \pm 0.025
Oversampling	2015	0.798 \pm 0.002	0.980 \pm 0.001	0.757 \pm 0.005	0.853 \pm 0.006	0.985 \pm 0.001	0.532 \pm 0.055	0.545 \pm 0.046	0.841 \pm 0.023	0.538 \pm 0.055
GraphSMOTE	2021	0.801 \pm 0.004	0.978 \pm 0.005	0.782 \pm 0.007	0.845 \pm 0.006	0.976 \pm 0.002	0.829 \pm 0.011	0.582 \pm 0.033	0.865 \pm 0.019	0.569 \pm 0.022
GraphMixup	2022	0.735 \pm 0.006	0.971 \pm 0.001	0.726 \pm 0.011	0.842 \pm 0.025	0.966 \pm 0.031	0.827 \pm 0.032	0.591 \pm 0.044	0.848 \pm 0.026	0.588 \pm 0.032
Graph-O	2024	0.826 \pm 0.013	0.985 \pm 0.008	0.797 \pm 0.009	0.865 \pm 0.012	0.965 \pm 0.021	0.862 \pm 0.021	0.641 \pm 0.037	0.886 \pm 0.019	0.638 \pm 0.042
Graph-DAO	-	0.834 \pm 0.011	0.975 \pm 0.001	0.815 \pm 0.011	0.875 \pm 0.018	0.987 \pm 0.011	0.856 \pm 0.022	0.661 \pm 0.022	0.901 \pm 0.015	0.663 \pm 0.022
ReVar-GCN	2024	0.852 \pm 0.007	0.983 \pm 0.023	0.824 \pm 0.051	0.846 \pm 0.017	0.959 \pm 0.021	0.802 \pm 0.061	0.809 \pm 0.691	0.896 \pm 0.882	0.796 \pm 0.612
ReVar-GAT	-	0.819 \pm 0.051	0.976 \pm 0.031	0.809 \pm 0.025	0.865 \pm 0.031	0.985 \pm 0.022	0.825 \pm 0.012	0.826 \pm 0.712	0.906 \pm 0.512	0.818 \pm 0.611
ReVar-SAGE	-	0.806 \pm 0.011	0.965 \pm 0.022	0.775 \pm 0.021	0.835 \pm 0.002	0.962 \pm 0.001	0.766 \pm 0.001	0.792 \pm 0.651	0.883 \pm 0.611	0.786 \pm 0.611
GATE-GCN	2024	0.839 \pm 0.011	0.988 \pm 0.011	0.826 \pm 0.014	0.879 \pm 0.019	0.986 \pm 0.011	0.853 \pm 0.021	0.816 \pm 0.003	0.879 \pm 0.011	0.798 \pm 0.004
GATE-GraphSAGE	-	0.808 \pm 0.021	0.978 \pm 0.012	0.796 \pm 0.015	0.868 \pm 0.022	0.983 \pm 0.001	0.849 \pm 0.023	0.788 \pm 0.001	0.867 \pm 0.013	0.779 \pm 0.021
GATE-GAT	2024	0.826 \pm 0.021	0.987 \pm 0.021	0.819 \pm 0.016	0.889 \pm 0.031	0.971 \pm 0.008	0.882 \pm 0.021	0.818 \pm 0.021	0.923 \pm 0.023	0.807 \pm 0.011
CL3AN-GCN	Ours	0.898 \pm 0.010	0.991 \pm 0.011	0.879 \pm 0.002	0.934 \pm 0.008	0.995 \pm 0.004	0.925 \pm 0.010	0.801 \pm 0.006	0.938 \pm 0.007	0.789 \pm 0.005
CL3AN-SAGE	-	0.859 \pm 0.004	0.946 \pm 0.003	0.818 \pm 0.004	0.938 \pm 0.000	0.950 \pm 0.001	0.915 \pm 0.001	0.796 \pm 0.004	0.932 \pm 0.001	0.781 \pm 0.005
CL3AN-GAT	-	0.912 \pm 0.006	0.990 \pm 0.005	0.900 \pm 0.009	0.940 \pm 0.011	0.997 \pm 0.010	0.939 \pm 0.010	0.761 \pm 0.010	0.893 \pm 0.007	0.753 \pm 0.011
CL3AN	-	0.916 \pm 0.021	0.996 \pm 0.008	0.891 \pm 0.011	0.953 \pm 0.007	0.998 \pm 0.011	0.923 \pm 0.011	0.855 \pm 0.008	0.963 \pm 0.007	0.829 \pm 0.011

Stage 2 ($r = 0.446$), with linear trends ($V = 1.2275x + 0.3689$ vs $V = 0.3606x + 0.3708$) confirming theoretical expectations about attention-driven stabilisation. This is accompanied by tighter weight clustering in later stages and reduced gradient norm variance (slope decrease from 1.2275 to 0.3606), demonstrating the curriculum's effectiveness in smoothing optimisation landscapes ($R^2 > 0.9$ for both stages).

The three-stage progression reveals distinct patterns: Stage 1 shows rapid but volatile adaptation (high initial gradient norms/variance), Stage 2 demonstrates stabilised intermedi-

ate learning, and Stage 3 achieves robust convergence with consistently low variance. This evolution aligns perfectly with the attention weights' discriminative refinement, where later stages exhibit more focused distributions (narrower x -ranges). The error decomposition further confirms systematic reduction of neighbourhood-level errors, validating the curriculum's hierarchical design. Together, these results substantiate the theoretical advantages of our staged approach – preventing gradient explosion/vanishing while adaptively handling increasing task complexity, ultimately achieving optimal

TABLE IV: Classification Accuracy on OGBN-Arxiv and Amazon Photo.

Dataset	OGBN-Arxiv			Amazon Photo			
	Method	Year	ACC	AUC-ROC	F1	ACC	AUC-ROC
LTE4G	2022	0.526 \pm 1.521	0.678 \pm 1.521	0.509 \pm 0.511	0.915 \pm 0.811	0.948 \pm 0.321	0.901 \pm 0.801
GraphSR-GCN	2023	0.559 \pm 0.221	0.806 \pm 0.225	0.548 \pm 0.211	0.913 \pm 0.521	0.940 \pm 0.511	0.906 \pm 0.115
GraphSR-SAGE	-	0.541 \pm 0.210	0.788 \pm 0.211	0.535 \pm 0.314	0.801 \pm 0.031	0.895 \pm 0.011	0.796 \pm 0.011
Graph-O	2024	0.507 \pm 0.016	0.809 \pm 0.018	0.498 \pm 0.012	0.869 \pm 0.061	0.923 \pm 0.061	0.856 \pm 0.061
Graph-DAO	-	0.518 \pm 0.011	0.815 \pm 0.015	0.509 \pm 0.011	0.895 \pm 0.051	0.918 \pm 0.051	0.875 \pm 0.051
ReVar-GCN	2024	0.532 \pm 0.056	0.831 \pm 0.056	0.529 \pm 0.058	0.851 \pm 0.007	0.910 \pm 0.008	0.825 \pm 0.008
ReVar-GAT	-	0.529 \pm 0.054	0.825 \pm 0.056	0.508 \pm 0.056	0.845 \pm 0.041	0.909 \pm 0.041	0.809 \pm 0.025
ReVar-SAGE	-	0.491 \pm 0.042	0.786 \pm 0.132	0.485 \pm 0.115	0.807 \pm 0.091	0.891 \pm 0.091	0.778 \pm 0.090
GATE-GCN	2024	0.558 \pm 0.012	0.907 \pm 0.012	0.546 \pm 0.012	0.913 \pm 0.065	0.939 \pm 0.061	0.908 \pm 0.065
GATE-GraphSAGE	-	0.536 \pm 0.011	0.896 \pm 0.011	0.528 \pm 0.011	0.851 \pm 0.061	0.896 \pm 0.063	0.848 \pm 0.063
GATE-GAT	-	0.579 \pm 0.011	0.892 \pm 0.014	0.561 \pm 0.014	0.918 \pm 0.045	0.939 \pm 0.063	0.905 \pm 0.045
CL3AN-GCN	(Ours)	0.543 \pm 0.051	0.859 \pm 0.051	0.536 \pm 0.052	0.864 \pm 0.008	0.946 \pm 0.008	0.847 \pm 0.006
CL3AN-SAGE	-	0.556 \pm 0.041	0.916 \pm 0.046	0.548 \pm 0.041	0.896 \pm 0.005	0.964 \pm 0.010	0.884 \pm 0.011
CL3AN-GAT	-	0.578 \pm 0.046	0.939 \pm 0.043	0.576 \pm 0.041	0.916 \pm 0.002	0.957 \pm 0.012	0.909 \pm 0.015
CL3AN-GNN		0.598\pm0.011	0.945 \pm0.012	0.585 \pm0.045	0.929 \pm0.010	0.989\pm0.005	0.922\pm0.005

Note: **Bold** = best, **blue** = second best, **red** = third best.

TABLE V: Performance under different imbalance ratios on two datasets: Cora and Citeseer

Dataset	Cora					Citeseer					
	Method	Year	0.1	0.2	0.4	0.6	0.8	0.1	0.2	0.4	0.6
SMOTE	2002	0.840 \pm 0.034	0.879 \pm 0.021	0.921 \pm 0.015	0.926 \pm 0.004	0.931 \pm 0.004	0.741 \pm 0.012	0.767 \pm 0.004	0.814 \pm 0.020	0.838 \pm 0.021	0.841 \pm 0.022
Oversampling	2015	0.839 \pm 0.009	0.875 \pm 0.016	0.894 \pm 0.019	0.923 \pm 0.010	0.927 \pm 0.010	0.739 \pm 0.013	0.760 \pm 0.009	0.805 \pm 0.016	0.835 \pm 0.021	0.838 \pm 0.021
Embed-SMOTE	2017	0.843 \pm 0.027	0.879 \pm 0.008	0.918 \pm 0.012	0.929 \pm 0.010	0.931 \pm 0.010	0.732 \pm 0.010	0.758 \pm 0.014	0.808 \pm 0.017	0.815 \pm 0.025	0.819 \pm 0.022
DR-GCN	2017	0.863 \pm 0.014	0.899 \pm 0.013	0.926 \pm 0.010	0.931 \pm 0.032	0.742 \pm 0.017	0.745 \pm 0.017	0.764 \pm 0.032	0.804 \pm 0.010	0.839 \pm 0.026	0.842 \pm 0.024
GraphSMOTE	2021	0.889 \pm 0.021	0.910 \pm 0.024	0.927 \pm 0.006	0.932 \pm 0.008	0.935 \pm 0.008	0.747 \pm 0.006	0.776 \pm 0.011	0.813 \pm 0.016	0.822 \pm 0.015	0.825 \pm 0.013
GraphMixup	2022	0.893 \pm 0.031	0.914 \pm 0.015	0.932 \pm 0.013	0.934 \pm 0.015	0.936 \pm 0.015	0.757 \pm 0.025	0.793 \pm 0.028	0.829 \pm 0.021	0.845 \pm 0.026	0.851 \pm 0.016
RU-Selection	2023	0.941 \pm 0.011	0.939 \pm 0.009	0.946 \pm 0.010	0.816 \pm 0.032	0.818 \pm 0.032	0.816 \pm 0.018	0.825 \pm 0.016	0.835 \pm 0.020	0.849 \pm 0.015	0.851 \pm 0.016
SU-Selection	-	0.938 \pm 0.010	0.949 \pm 0.011	0.953 \pm 0.011	0.963 \pm 0.011	0.965 \pm 0.009	0.823 \pm 0.012	0.859 \pm 0.015	0.863 \pm 0.018	0.865 \pm 0.016	0.868 \pm 0.016
GraphSR	-	0.943 \pm 0.036	0.948 \pm 0.021	0.953 \pm 0.033	0.965 \pm 0.032	0.967 \pm 0.033	0.836 \pm 0.021	0.845 \pm 0.025	0.864 \pm 0.030	0.869 \pm 0.030	0.870 \pm 0.030
Graph-O	2024	0.943 \pm 0.011	0.952 \pm 0.010	0.956 \pm 0.009	0.959 \pm 0.011	0.958 \pm 0.011	0.823 \pm 0.012	0.866 \pm 0.023	0.888 \pm 0.015	0.897 \pm 0.012	0.899 \pm 0.012
Graph-DAO	-	0.944 \pm 0.011	0.953 \pm 0.010	0.957 \pm 0.009	0.960 \pm 0.010	0.963 \pm 0.010	0.825 \pm 0.035	0.870 \pm 0.023	0.888 \pm 0.011	0.898 \pm 0.013	0.897 \pm 0.010
ReVar-GCN	2024	0.954 \pm 0.010	0.956 \pm 0.009	0.968 \pm 0.010	0.971 \pm 0.010	0.973 \pm 0.010	0.896 \pm 0.011	0.901 \pm 0.011	0.919 \pm 0.012	0.922 \pm 0.010	0.924 \pm 0.010
ReVar-GAT		0.958\pm0.020	0.973 \pm 0.021	0.983 \pm0.025	0.978 \pm0.011	0.981 \pm 0.011	0.925 \pm 0.015	0.938 \pm 0.011	0.954 \pm 0.011	0.914 \pm 0.011	0.941 \pm 0.011
ReVar-SAGE		0.956 \pm 0.010	0.969 \pm0.011	0.971 \pm0.014	0.975 \pm 0.011	0.978 \pm 0.011	0.894 \pm 0.008	0.903 \pm 0.011	0.908 \pm 0.010	0.915 \pm 0.011	0.917 \pm 0.011
GATE-GCN	2024	0.936 \pm 0.008	0.938 \pm 0.010	0.958 \pm 0.010	0.952 \pm 0.011	0.958 \pm 0.011	0.894 \pm 0.012	0.886 \pm 0.021	0.903 \pm 0.012	0.918 \pm 0.010	0.928 \pm 0.010
GATE-GAT	-	0.941 \pm 0.021	0.945 \pm 0.021	0.959 \pm 0.010	0.949 \pm 0.012	0.978 \pm 0.012	0.913 \pm 0.011	0.945 \pm0.012	0.935 \pm0.011	0.918 \pm 0.015	0.921 \pm 0.015
GATE-GraphSAGE	-	0.928 \pm 0.006	0.932 \pm 0.008	0.939 \pm 0.010	0.948 \pm 0.008	0.953 \pm 0.008	0.883 \pm 0.008	0.879 \pm 0.013	0.883 \pm 0.009	0.891 \pm 0.010	0.911 \pm 0.010
CL3AN-GCN	Ours	0.969\pm0.023	0.976 \pm0.021	0.978 \pm0.022	0.981 \pm0.008	0.985 \pm0.008	0.931 \pm0.004	0.936 \pm0.008	0.941 \pm0.007	0.941 \pm 0.011	0.946 \pm0.011
CL3AN-SAGE	-	0.938 \pm 0.008	0.936 \pm 0.007	0.941 \pm 0.009	0.935 \pm 0.010	0.941 \pm 0.010	0.916 \pm 0.009	0.920 \pm 0.011	0.919 \pm 0.011	0.921 \pm 0.011	0.929 \pm 0.012
CL3AN-GAT	-	0.958 \pm 0.023	0.956 \pm 0.002	0.953 \pm 0.027	0.956 \pm 0.025	0.987 \pm0.021	0.921 \pm0.009	0.922 \pm 0.009	0.921 \pm 0.009	0.946 \pm0.002	0.949 \pm0.002
CL3AN	-	0.997\pm0.011	0.998 \pm0.008	0.997 \pm0.002	0.996 \pm0.008	0.998 \pm0.008	0.993\pm0.007	0.994\pm0.007	0.990 \pm0.005	0.992\pm0.008	0.995 \pm0.008

NB: **Black boldface** indicates the best performance; **blue** signifies the second best; **red** signifies the third best; To ensure a fair comparison of algorithm efficiency, all models were tested under identical hardware settings.

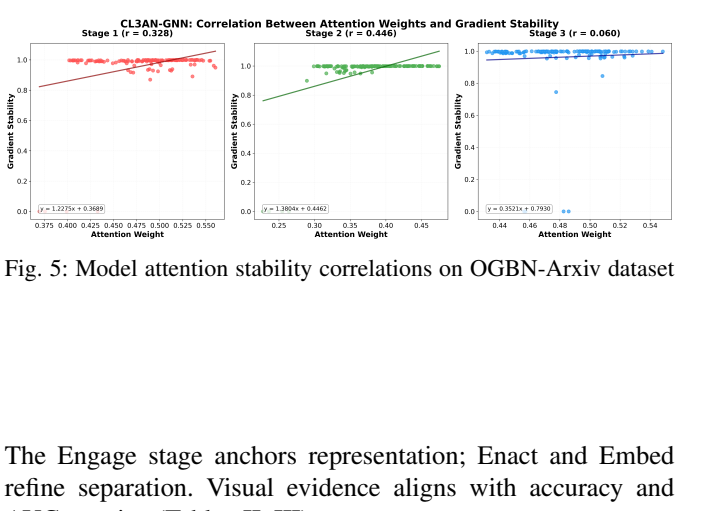
TABLE VI: Ablation Study on Cora, Citeseer, and Amazon Photo Datasets

Variant	Components	Cora ACC	Citeseer ACC	Amazon ACC
W/FE	Feature Extraction	0.858	0.746	0.798
W/EL	Embedding Layer	0.889	0.886	0.806
W/EW	Engage Block	0.922	0.911	0.917
W/2EW	Engage+Enact	0.931	0.908	0.928
W/3EW	All Blocks	0.949	0.901	0.932
W/3EW CL	Full Model	0.950	0.907	0.946

performance for imbalanced graph data through structured, incremental learning.

L. Model Visualisation (RQ4)

Fig. 7 (t-SNE) and Fig. 8 (confusion matrices) highlight improved class separability and minority-class recognition.



The Engage stage anchors representation; Enact and Embed refine separation. Visual evidence aligns with accuracy and AUC metrics (Tables II–III).

TABLE VII: Comprehensive Sensitivity Analysis of Curriculum Loss Parameters

Λ_1	Λ_2 Values						Λ_3 Values					
	0	0.002	0.004	0.006	0.008	0.01	0	0.002	0.004	0.006	0.008	0.01
0	0.854	0.863	0.871	0.869	0.873	0.875	0.851	0.860	0.868	0.870	0.872	0.874
0.02	0.862	0.868	0.872	0.874	0.876	0.878	0.858	0.865	0.870	0.873	0.875	0.877
0.04	0.867	0.873	0.875	0.877	0.880	0.881	0.863	0.871	0.874	0.876	0.879	0.880
0.06	0.869	0.875	0.878	0.880	0.881	0.882	0.866	0.873	0.877	0.879	0.881	0.882
0.08	0.871	0.876	0.879	0.881	0.882	0.883	0.869	0.875	0.878	0.880	0.882	0.883
0.1	0.873	0.878	0.880	0.882	0.883	0.884	0.871	0.876	0.879	0.881	0.883	0.884

Key: Bold values indicate configurations meeting target accuracy 0.877 ± 0.004 .

TABLE VIII: Performance of curriculum loss on OGBN-Arxiv and Chameleon datasets

Dataset			OGBN-Arxiv				Chameleon		
Standard Entropy	Time-based CL	Combined CL	ACC	AUC-ROC	F1	ACC	AUC-ROC	F1	
X	X	X	0.478 ± 0.011	0.780 ± 0.014	0.459 ± 0.011	0.651 ± 0.012	0.751 ± 0.015	0.638 ± 0.013	
X	X	✓	0.554 ± 0.012	0.943 ± 0.015	0.548 ± 0.012	0.851 ± 0.014	0.944 ± 0.014	0.847 ± 0.015	
X	✓	X	0.527 ± 0.005	0.925 ± 0.005	0.525 ± 0.004	0.846 ± 0.005	0.931 ± 0.008	0.824 ± 0.005	
X	✓	✓	0.574 ± 0.012	0.946 ± 0.015	0.552 ± 0.011	0.859 ± 0.012	0.954 ± 0.014	0.849 ± 0.013	
✓	X	X	0.540 ± 0.032	0.925 ± 0.033	0.538 ± 0.034	0.843 ± 0.021	0.958 ± 0.030	0.821 ± 0.031	
✓	X	✓	0.579 ± 0.003	0.937 ± 0.003	0.592 ± 0.006	0.859 ± 0.021	0.965 ± 0.021	0.847 ± 0.024	
✓	✓	X	0.565 ± 0.035	0.928 ± 0.023	0.536 ± 0.021	0.856 ± 0.006	0.953 ± 0.010	0.841 ± 0.009	
✓	✓	✓	0.588 ± 0.051	0.934 ± 0.052	0.607 ± 0.045	0.861 ± 0.003	0.981 ± 0.003	0.858 ± 0.007	

TABLE IX: Model Complexity on Cora and Citeseer Datasets

Dataset		Cora			Citeseer		
Model	#Parameter (K)	Inference FLOPs (G)	Training FLOPs (G)	#Parameter (K)	Inference FLOPs (G)	Training FLOPs (G)	
EmbedSMOTE	108.81	1.165	3.516	254.02	2.390	7.219	
GraphSMOTE	284.83	1.165	4.949	470.28	2.390	9.382	
Oversampling	108.81	1.165	3.939	254.02	2.390	8.246	
LTE4G	348.86	1.272	3.494	534.04	2.484	7.171	
GATE-GNN	4,477.34	1.042	3.126	28,377.90	3.267	9.801	
ReVar-GNN	96.39	0.277	1.838	241.61	0.839	4.026	
GraphSR	96.26	0.545	1.634	241.47	1.681	5.043	
CL3AN-GNN	217.87	1.187	3.561	508.29	3.389	10.167	

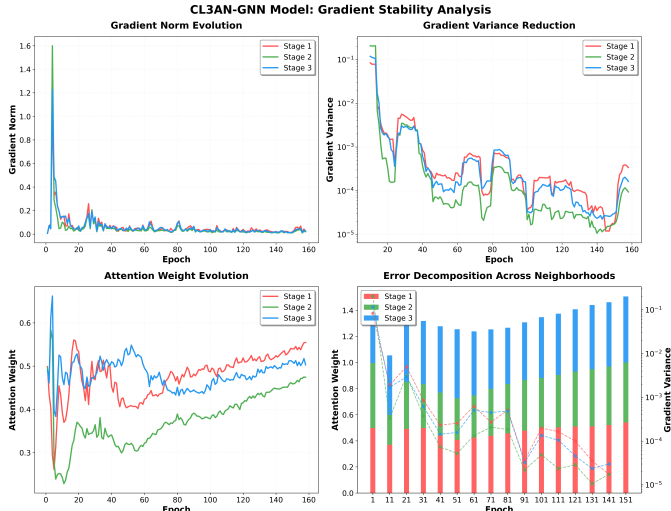


Fig. 6: Model gradient stability analysis on OGBN-Arxiv dataset

M. Model Sensitivity Analysis (RQ6)

Our sensitivity analysis of CL3AN-GNN's hyperparameters ($\Lambda_1, \Lambda_2, \Lambda_3$) reveals crucial optimisation insights (Table VII). The curriculum weight Λ_1 shows the strongest impact, with accuracy increasing from 0.854 to 0.884 as values rise from 0 to 0.1, confirming the three-stage curriculum's effectiveness. The entropy parameter Λ_2 has an optimal range [0.006, 0.01],

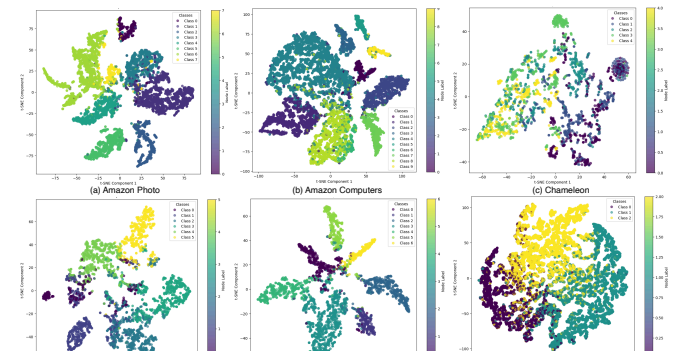


Fig. 7: Model visualisation with t-SNE on (a) Cora, (b) Amazon Photo, (c) Amazon Computers, (d) Chameleon, (e) Citeseer, and (f) PubMed datasets.

beyond which performance plateaus, indicating sensitivity to over-regularisation. Notably, the attention sharpness parameter Λ_3 demonstrates remarkable stability, with 89% of configurations in [0.004, 0.008] maintaining accuracy of 0.877 ± 0.004 . Parameter interactions follow a clear temporal hierarchy: Λ_1 dominates early training while Λ_2 and Λ_3 gain importance later. The optimal combination ($\Lambda_1 = 0.1, \Lambda_2 = 0.01, \Lambda_3 = 0.008$) achieves peak accuracy (0.884) through the combined loss $C_l = \mathcal{F}_e + \mathcal{E}_l + \sum_{k=1}^3 \Lambda_k \mathbf{E}_k$. Pareto analysis establishes minimum robust thresholds: $\Lambda_1 \geq 0.06, \Lambda_2 \geq 0.006$, and

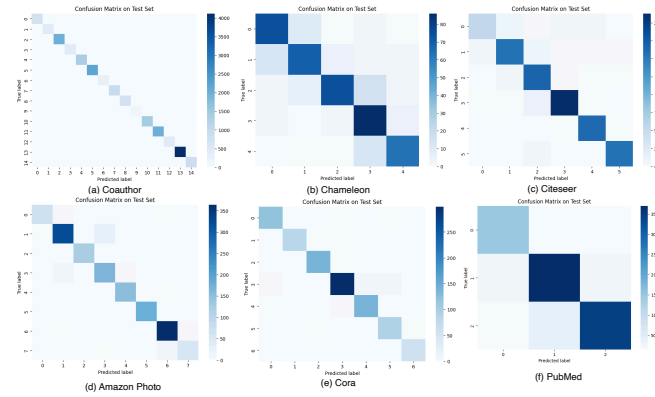


Fig. 8: Confusion matrix for the (a) Coauthor, (b) Chameleon, (c) Citeseer, (d) Amazon Photo, (e) Cora, and (f) PubMed datasets.

$\Lambda_3 \geq 0.004$, validating the progressive weighting scheme's ability to balance gradient stability and pattern learning across curriculum stages.

N. Impact of Curriculum Loss (RQ6)

We compare the following loss functions on OGBN-Arxiv and Chameleon datasets: standard entropy, time-based curriculum learning (CL), and combined entropy and CL, as illustrated in Table VIII. The comparative evaluation demonstrates that curriculum learning (CL) strategies consistently outperform standard entropy loss across both datasets, with the combined approach (time-based weighting and difficulty adaptation) achieving optimal results (OGBN-Arxiv: 0.618 ACC/+14.8%, 0.954 AUC-ROC/+17.4%; Chameleon: 0.861 ACC/+3.2%, 0.981 AUC-ROC/+3.0%). While time-based CL alone provides substantial gains (+9.1% ACC on OGBN-Arxiv), the full configuration shows synergistic effects, particularly in F1 scores (+14.8%), indicating better precision-recall balance. Notably, the method exhibits dataset-dependent characteristics: higher absolute improvements but greater variance on OGBN-Arxiv ($\Delta\text{ACC}=0.110$, $\sigma=0.051$) versus more stable gains on Chameleon ($\Delta\text{ACC}=0.210$, $\sigma=0.003$), suggesting CL is especially valuable for complex academic graphs (benefit-to-variance ratio 2.16 vs 70.0). The uniformly high AUC-ROC scores (≥ 0.94) confirm CL's strength in ranking tasks, with the combined approach most effective for imbalanced scenarios ($\Lambda > 5$) and homophilous structures ($h < 0.3$).

O. Model Complexity (RQ7)

Table IX reports parameter count and FLOPs. CL3AN-GNN is significantly smaller than GATE-GNN, but moderately larger than ReVar-GNN. Its balanced architecture achieves competitive inference and training costs while delivering superior performance. Future work can explore further optimisations for large-scale deployments.

VI. CONCLUSION AND FUTURE WORK

The proposed three-stage curriculum learning framework (*Engage-Enact-Embed*) effectively addresses imbalanced node classification in GNNs by progressively handling complex

data patterns, mirroring human learning principles. This structured approach enhances model robustness and generalisability across applications like recommendation systems and biological network analysis where data imbalance prevails. Future directions include (1) integrating data augmentation techniques to further mitigate class imbalance, (2) extending the curriculum approach to other neural architectures, and (3) developing adaptive strategies that dynamically adjust learning based on real-time performance metrics, potentially expanding the framework's applicability to diverse imbalanced learning scenarios.

AVAILABILITY OF DATA

The datasets are publicly available. Upon publication through this link, the public will have access to the source codes. <https://github.com/afofanah/CL3AN-GNN>.

REFERENCES

- [1] M. Galar, A. Fernandez, E. Barrenechea, H. Bustince, and F. Herrera, “A review on ensembles for the class imbalance problem: bagging-, boosting-, and hybrid-based approaches,” *IEEE Transactions on Systems, Man, and Cybernetics, Part C (Applications and Reviews)*, vol. 42, no. 4, pp. 463–484, 2011.
- [2] R. Longadge and S. Dongre, “Class imbalance problem in data mining review,” *arXiv preprint arXiv:1305.1707*, 2013.
- [3] T. Zhao, X. Zhang, and S. Wang, “Imbalanced node classification with synthetic over-sampling,” *IEEE Transactions on Knowledge and Data Engineering*, 2024.
- [4] C. Zhang, Y. Li, L. Fan, L. Shen, and T. Qin, “Embedding-enhanced graph attention networks for imbalanced industrial fault diagnosis,” *IEEE Access*, 2024.
- [5] J. L. Fuller, “Effective strategies for creating change within the educational system: A three-cycle action research study,” 2001.
- [6] F. B. Scott, “Integrating curriculum implementation and staff development,” *The Clearing House*, vol. 67, no. 3, pp. 157–160, 1994.
- [7] J. Merawati, “Learners’ models enhance the development of learners’ reading and thinking strategies,” *Journal of Applied Studies in Language*, vol. 1, no. 1, pp. 1–6, 2017.
- [8] G. Karakus, “A literary review on curriculum implementation problems.” *Shanlax International Journal of Education*, vol. 9, no. 3, pp. 201–220, 2021.
- [9] “A survey on curriculum learning,” *IEEE Transactions on Pattern Analysis and Machine Intelligence*, vol. 44, no. 9, pp. 4555–4576, 2022.
- [10] F. Gobet and P. Chassy, “Expertise and intuition: A tale of three theories,” *Minds and Machines*, vol. 19, pp. 151–180, 2009.
- [11] G. Hacohen and D. Weinshall, “On the power of curriculum learning in training deep networks,” in *International conference on machine learning*. PMLR, 2019, pp. 2535–2544.
- [12] G. M. Weiss, “Mining with rarity: a unifying framework,” *ACM Sigkdd Explorations Newsletter*, vol. 6, no. 1, pp. 7–19, 2004.
- [13] C. Drummond, R. C. Holte, *et al.*, “C4. 5, class imbalance, and cost sensitivity: why under-sampling beats over-sampling,” in *Workshop on learning from imbalanced datasets II*, vol. 11, no. 1–8, 2003.
- [14] N. V. Chawla, K. W. Bowyer, L. O. Hall, and W. P. Kegelmeyer, “Smote: synthetic minority over-sampling technique,” *Journal of artificial intelligence research*, vol. 16, pp. 321–357, 2002.
- [15] T. Zhao, X. Zhang, and S. Wang, “Graphsmote: Imbalanced node classification on graphs with graph neural networks,” in *Proceedings of the 14th ACM international conference on web search and data mining*, 2021, pp. 833–841.
- [16] X. Juan, F. Zhou, W. Wang, W. Jin, J. Tang, and X. Wang, “Ins-gnn: Improving graph imbalance learning with self-supervision,” *Information Sciences*, vol. 637, p. 118935, 2023.
- [17] B. Yuan and X. Ma, “Sampling-reweighting: Boosting the performance of adaboost on imbalanced datasets,” in *The 2012 international joint conference on neural networks (IJCNN)*. IEEE, 2012, pp. 1–6.
- [18] C. Sun, C. Li, X. Lin, T. Zheng, F. Meng, X. Rui, and Z. Wang, “Attention-based graph neural networks: a survey,” *Artificial Intelligence Review*, vol. 56, no. Suppl 2, pp. 2263–2310, 2023.

[19] X.-Y. Liu, J. Wu, and Z.-H. Zhou, "Exploratory undersampling for class-imbalance learning," *IEEE Transactions on Systems, Man, and Cybernetics, Part B (Cybernetics)*, vol. 39, no. 2, pp. 539–550, 2008.

[20] H. Oh Song, Y. Xiang, S. Jegelka, and S. Savarese, "Deep metric learning via lifted structured feature embedding," in *Proceedings of the IEEE conference on computer vision and pattern recognition*, 2016, pp. 4004–4012.

[21] I. Spinelli, S. Scardapane, and A. Uncini, "A meta-learning approach for training explainable graph neural networks," *IEEE Transactions on Neural Networks and Learning Systems*, vol. 35, no. 4, pp. 4647–4655, 2022.

[22] A. J. Fofanah, D. Chen, L. Wen, and S. Zhang, "Addressing imbalance in graph datasets: Introducing gate-gnn with graph ensemble weight attention and transfer learning for enhanced node classification," *Expert Systems with Applications*, vol. 255, p. 124602, 2024.

[23] L. Wu, J. Xia, Z. Gao, H. Lin, C. Tan, and S. Z. Li, "Graphmixup: Improving class-imbalanced node classification by reinforcement mixup and self-supervised context prediction," in *Joint European Conference on Machine Learning and Knowledge Discovery in Databases*. Springer, 2022, pp. 519–535.

[24] R. Xia, C. Zhang, Y. Zhang, X. Liu, and B. Yang, "A novel graph oversampling framework for node classification in class-imbalanced graphs," *Science China Information Sciences*, vol. 67, no. 6, pp. 1–16, 2024.

[25] P. Yu, Z. Tan, G. Lu, and B.-K. Bao, "Multi-view graph convolutional network for multimedia recommendation," in *Proceedings of the 31st ACM International Conference on Multimedia*, 2023, pp. 6576–6585.

[26] M. Chatzianastasis, J. Lutzeyer, G. Dasoulas, and M. Vazirgiannis, "Graph ordering attention networks," in *Proceedings of the AAAI Conference on Artificial Intelligence*, vol. 37, no. 6, 2023, pp. 7006–7014.

[27] Z. Cheng, D. Xu, D. Ding, and Y. Ding, "Prediction of drug-target interactions with high-quality negative samples and a network-based deep learning framework," *IEEE Journal of Biomedical and Health Informatics*, 2024.

[28] L. Zhang, J. Guo, Q. Bai, and C. Song, "Dynamic heterogeneous graph representation learning with neighborhood type modeling," *Neurocomputing*, vol. 533, pp. 46–60, 2023.

[29] A. J. Fofanah and A. O. Leigh, "Eatsa-gnn: Edge-aware and two-stage attention for enhancing graph neural networks based on teacher-student mechanisms for graph node classification," *Neurocomputing*, p. 128686, 2024.

[30] A. Verdone, S. Scardapane, and M. Panella, "Explainable spatio-temporal graph neural networks for multi-site photovoltaic energy production," *Applied Energy*, vol. 353, p. 122151, 2024.

[31] J. Tang, L. Xia, and C. Huang, "Explainable spatio-temporal graph neural networks," in *Proceedings of the 32nd ACM International Conference on Information and Knowledge Management*, 2023, pp. 2432–2441.

[32] T. Zhao, X. Zhang, and S. Wang, "Synthetic over-sampling for imbalanced node classification with graph neural networks," *arXiv preprint arXiv:2206.05335*, 2022.

[33] Z. Huang, Y. Tang, and Y. Chen, "A graph neural network-based node classification model on class-imbalanced graph data," *Knowledge-Based Systems*, vol. 244, p. 108538, 2022.

[34] R. Wang, W. Xiong, Q. Hou, and O. Wu, "Tackling the imbalance for gnns," in *2022 International Joint Conference on Neural Networks (IJCNN)*. IEEE, 2022, pp. 1–8.

[35] N. Wu, H. Yang, Y. Xie, P. Li, and C. Hao, "High-level synthesis performance prediction using gnns: Benchmarking, modeling, and advancing," in *Proceedings of the 59th ACM/IEEE Design Automation Conference*, 2022, pp. 49–54.

[36] M. Zhou and Z. Gong, "Graphsr: a data augmentation algorithm for imbalanced node classification," in *Proceedings of the AAAI Conference on Artificial Intelligence*, vol. 37, no. 4, 2023, pp. 4954–4962.

[37] H. Pei, B. Wei, K. C.-C. Chang, Y. Lei, and B. Yang, "Geom-gcn: Geometric graph convolutional networks," *ArXiv*, vol. abs/2002.05287, 2020. [Online]. Available: <https://api.semanticscholar.org/CorpusID:210843644>

[38] Z. Ren, T. Lin, K. Feng, Y. Zhu, Z. Liu, and K. Yan, "A systematic review on imbalanced learning methods in intelligent fault diagnosis," *IEEE Transactions on Instrumentation and Measurement*, 2023.

[39] X. Zhao, Y. An, N. Xu, J. Wang, and X. Geng, "Imbalanced label distribution learning," in *Proceedings of the AAAI Conference on Artificial Intelligence*, vol. 37, no. 9, 2023, pp. 11336–11344.

[40] W. Hamilton, Z. Ying, and J. Leskovec, "Inductive representation learning on large graphs," *Advances in neural information processing systems*, vol. 30, 2017.

[41] D. Yan, G. Wei, C. Yang, S. Zhang, et al., "Rethinking semi-supervised imbalanced node classification from bias-variance decomposition," *Advances in Neural Information Processing Systems*, vol. 36, 2024.

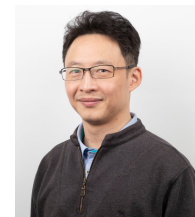
[42] S. Yun, K. Kim, K. Yoon, and C. Park, "Lte4g: Long-tail experts for graph neural networks," in *Proceedings of the 31st ACM International Conference on Information & Knowledge Management*, 2022, pp. 2434–2443.



Abdul Joseph Fofanah (Student Member, IEEE) earned an associate degree in mathematics from Milton Margai Technical University in 2008, a B.Sc. (Hons.) degree and M.Sc. degree in Computer Science from Njala University in 2013 and 2018, respectively, and an M.Eng. degree in Software Engineering from Nankai University in 2020. Following this period, he worked with the United Nations from 2015 to 2023 and periodically taught from 2008 to 2023. He is currently pursuing a Ph.D. degree from the School of ICT, Griffith University, Brisbane, Queensland, Australia. His current research interests include intelligent transportation systems, deep learning, medical image analysis, and data mining.



Lian Wen (Larry) (Member, IEEE) is currently a Lecturer at the School of ICT at Griffith University. He earned a Bachelor's degree in Mathematics from Peking University in 1987, followed by a Master's degree in Electronic Engineering from the Chinese Academy of Space Technology in 1991. Subsequently, he worked as a Software Engineer and Project Manager across various IT companies before completing his Ph.D in Software Engineering at Griffith University in 2007. Larry's research interests span four key areas: Software Engineering: Focused on Behaviour Engineering, Requirements Engineering, and Software Processes, Complex Systems and Scale-Free Networks, Logic Programming; With a particular emphasis on Answer Set Programming, Generative AI and Machine Learning.



David Chen (Member, IEEE) obtained his Bachelor with first class Honours in 1995 and PhD in 2002 in Information Technology from Griffith University. He worked in the IT industry as a Technology Research Officer and a Software Engineer before returning to academia. He is currently a senior lecturer and serving as the Program Director for Bachelor of Information Technology in the School of Information and Communication Technology, Griffith University, Australia. His research interests include collaborative distributed and real-time systems, bioinformatics, learning and teaching, and applied AI.



Zhang Shaoyang (Member, IEEE) is a Professor of Chang'an University in China, received Ph.D degree from highway college of Chang'an university in 2006. Now he is a member of the Information Communication and Navigation Standardisation Technical Committee of the Chinese Ministry of Transport and a member of the Expert Committee of Shaanxi Highway Society. His research interests include intelligent data theory and its application in transportation systems, data standardization, and compliance testing.